International Journal of Bifurcation and Chaos, Vol. 15, No. 8 (2005) 2395–2409

SEMI-ANALYTICAL BIFURCATION ANALYSIS OF TWO-PHASE FLOW IN A HEATED CHANNEL

A. DOKHANE*,†, D. HENNIG and R. CHAWLA*
Laboratory for Reactor Physics and Systems Behavior,
Paul Scherrer Institute, CH-5232 Villigen, Switzerland
**Swiss Federal Institute of Technology (EPFL)*
PHB-Ecublens, CH-1015 Lausanne, Switzerland
†*Abdelhamid.dokhane@psi.ch*

RIZWAN-UDDIN
Department of Nuclear, Plasma, and Radiological Engineering,
University of Illinois,
103 S. Goodwin Ave. Urbana, IL 61801, USA

Received July 2, 2004; Revised October 22, 2004

Using a drift flux representation for the two-phase flow, a new reduced order model has been developed to simulate density-wave oscillations (DWOs) in a heated channel. This model is then used to perform stability and semi-analytical bifurcation analysis, using the bifurcation code BIFDD, in which the stability boundary (SB) and the nature of Hopf bifurcation are determined in a suitable two-dimensional parameter space.

A comparative study is carried out to investigate the effects of the parameters in the drift flux model (DFM) — the radially void distribution parameter C_0 and the drift velocity V_{gj} — on the SB as well as on the nature of Hopf bifurcation. It is the first time that a systematic analysis has been carried out to investigate the effects of DFM parameters on the nature of Hopf bifurcation in a heated-channel two-phase flow.

The results obtained show that both sub- and super-critical Hopf bifurcations are encountered. In addition, it has been found that, while the SB is sensitive to both C_0 and V_{gj}, the nature of Hopf bifurcation for lower values of N_{sub} is more sensitive to V_{gj} than to C_0. Numerical integration of the set of ODEs is carried out to confirm the predictions of the semi-analytical bifurcation analysis.

Keywords: Hopf bifurcation; stability; two-phase flow; drift flux.

1. Introduction

Nonlinear boiling water reactor (BWR) studies are generally pursued by employing large system codes like RAMONA [Wulf *et al.*, 1984] and RETRAN [Jensen & Galer, 1990]. However, detailed investigations using this approach, where parametric studies are to be carried out over large regions of parameter space, are very expensive and time consuming. For this purpose, it is necessary to use the so-called reduced order models containing a "manageable" number of system equations incorporating the essential features of the physical phenomena involved. Since the thermal-hydraulic model determines the main feedback gain and the associated time delay (void feedback reactivity), the modeling of the fluid dynamics is of paramount importance in the

†Author for correspondence.

reduced order model analysis of BWRs. For a certain set of hydraulic parameter values, the system of nonlinear differential equations describing the fluid dynamics can generate so-called self-sustained density-wave oscillations (DWOs), a typical two-phase flow instability.

The study of the nonlinear behavior of density wave instabilities has attracted considerable interest in the last two decades. Benefiting from the development of nonlinear dynamics theory, significant advances have been made in the nonlinear stability analysis of heated channels as well as BWRs. Moreover, additional efforts have been recently concentrated on bifurcation analyses, in which the effects of different design as well as operational parameters on bifurcation characteristics are analyzed. Such bifurcation analyses give important information that should be taken into account in the design and operational analysis of the next generation of BWRs.

Achard *et al.* [1985] carried out an analytical bifurcation study of DWO phenomena on the basis of a homogeneous equilibrium model (HEM). This led to two functional differential equations (FDEs). Rizwan-uddin and Dorning [1986] extended that model using a drift flux model and obtained very complicated nonlinear, functional, delay, integro-differential equations for the inlet velocity and two-phase residence time. They carried out stability and bifurcation analyses and showed that the SB is sensitive to the value of C_0 (void radial distribution parameter). The effect of V_{gj} (drift velocity) on the SB appeared to be small. The nature of Hopf bifurcation along the entire SB was found to be supercritical. However, the impact of C_0 and V_{gj} on the nature of Hopf bifurcation was not reported.

Later, starting from the homogeneous equilibrium model, Clausse and Lahey [1991] developed a simple model for DWOs by introducing some simplifying assumptions, such as simple linear approximations for the space dependence of the enthalpies in the single-phase and two-phase regions.

In the spirit of these developments, Karve *et al.* [1994] developed a model (using HEM) based on the assumptions that the time-dependent single-phase enthalpy and two-phase quality have spatially quadratic profiles. This model is simple in that the dynamical system that results is comprised of a set of nonlinear ODEs rather than complicated FDEs. After stability analyses for the stability boundary, they carried out bifurcation analyses entirely numerically [Karve *et al.*, 1997].

It should be emphasized that all the previous studies mentioned above applied either pure analytical, or pure numerical,[1] bifurcation analysis. Pure analytical bifurcation needs extensive mathematical manipulation and become almost impossible to carry out for higher order models. Moreover, this type of bifurcation analysis can be carried out only for one specific bifurcation parameter at a time, and must be repeated if the impact of different parameters is to be studied. On the other hand, numerical bifurcation can only be performed for a limited number of operational points. Hence, due to the limitations of these two approaches, the scope of these previous analyses was limited to a small region of the rather large parameter space, in spite of the simplicity of the models used.

In the present paper, using the same assumptions as in the Karve *et al.* model, we develop a model based on a drift flux representation for the two-phase flow. Such a model is more appropriate, since it takes into account: (a) the difference between the two-phase velocities, which is particularly important in low-flow regimes, and (b) the radially nonuniform void distribution inside the channel. Moreover, we perform stability and so-called *semi-analytical* bifurcation (see Sec. 3) analyses using the bifurcation analysis code BIFDD [Hassard, 1987]. In effect, to the authors' knowledge, this is the first time that a systematic analysis has been carried out to investigate the effects of DFM parameters on the nature of Hopf bifurcation in a heated channel two-phase flow problem.

This paper is organized in the following way. The next section presents the derivation of the heated channel model. In Sec. 3, the mathematical background of Hopf bifurcation is briefly reviewed, and semi-analytical bifurcation analysis and the code BIFDD are described. Section 4 is devoted to a comparison between the use of the drift flux and homogeneous equilibrium models, using both semi-analytical bifurcation analysis and standard numerical integration of the sets of ODEs. Finally, a summary and conclusion of the present work are given in the last section.

[1]Numerical integration.

2. Model

Using the drift flux model to represent the two-phase flow, the mathematical model is based on the assumptions that the single-phase enthalpy and the two-phase quality have spatially quadratic but time-dependent profiles. These assumptions have been used earlier with the homogeneous equilibrium model for two-phase flow [Karve *et al.*, 1994].

Five ODEs result from the integration of the one-dimensional time-dependent continuity, energy and momentum equations in the single- and two-phase regions using a weighted residuals procedure. The integration is carried out analytically using the Maple symbolic toolbox. The Roman and Greek symbols are defined in the nomenclature section, and the details of the dimensionless variables and parameters are given in Appendix A.

2.1. *Single-phase region*

The single-phase region extends from the channel inlet to the boiling boundary $\mu(t)$ (see Fig. 1), i.e. the location where bulk boiling begins. The energy equation can be written in dimensionless form as follows:

$$\frac{\partial h(z,t)}{\partial t} + v_{\text{inlet}}(t)\frac{\partial h(z,t)}{\partial z} = N_\rho N_r N_{\text{pch},1\phi}(t) \quad (1)$$

where $h(z,t)$ is the single-phase enthalpy, $v_{\text{inlet}}(t)$ is the liquid inlet velocity, and $N_{\text{pch},1\phi}(t)$ is the time-dependent phase-change number in the single-phase region, which is proportional to the heat flux in the single-phase region. The dimensionless quantities N_ρ and N_r are defined in Appendix A.

A time-dependent, spatially quadratic distribution for the enthalpy, as originally proposed and validated by Karve *et al.* [1994], is now introduced:

$$h(z,t) \approx h_{\text{inlet}} + a_1(t)z + a_2(t)z^2 \quad (2)$$

Substituting this expression in the single-phase energy equation (1), using weight functions 1 and z, and integrating from the inlet of the channel $z = 0$ to the boiling boundary $z = \mu(t)$, we arrive at the ODEs for the phase variables $a_1(t)$ and $a_2(t)$ for the single-phase region:

$$\frac{da_1(t)}{dt} = \frac{6}{\mu(t)}[N_\rho N_r N_{\text{pch},1\phi}(t) - v_{\text{inlet}}(t)a_1(t)] - 2v_{\text{inlet}}(t)a_2(t), \quad (3)$$

$$\frac{da_2(t)}{dt} = \frac{6}{\mu^2(t)}[N_\rho N_r N_{\text{pch},1\phi}(t) - v_{\text{inlet}}(t)a_1(t)] \quad (4)$$

2.2. *Two-phase region*

The two-phase region extends from the boiling boundary to the channel exit as shown in Fig. 1. Derived from the four fundamental equations [Zuber & Staub, 1967], the drift flux equations for two-phase flow in the dimensionless form are [Rizwan-uddin & Dorning, 1986]:

$$\frac{\partial j(z,t)}{\partial t} = N_{\text{pch},2\phi}(t), \quad (5)$$

$$\frac{\partial \alpha(z,t)}{\partial t} + (C_0 j(z,t) + V_{gj})\frac{\partial \alpha(z,t)}{\partial z} = N_{\text{pch},2\phi}(t)[N_r - C_0\alpha(z,t)] \quad (6)$$

for the conservation of volumetric flux and void fraction, and

$$-\frac{\partial P_{2\phi}}{\partial z} = \rho_m(z,t)\left[Fr^{-1} + \frac{\partial \mathrm{v}_m(z,t)}{\partial t} + \mathrm{v}_m(z,t)\frac{\partial \mathrm{v}_m(z,t)}{\partial z} + N_{f,2\phi}v_m^2(z,t)\right] + \mathrm{N}_\rho\,\frac{\partial}{\partial z}\left(\frac{\alpha}{1-\alpha}\frac{\overline{V}_{gj}^2}{\rho_m(z,t)}\right) \quad (7)$$

for the conservation of momentum of the mixture, with the different quantities defined as follows:

$\overline{V}_{gj} = V_{gj} + (C_0 - 1)\cdot j(z,t)$, where V_{gj} is the drift velocity, C_0 is the radially void distribution parameter, and $j(z,t) = \mathrm{v}_{\text{inlet}}(t) + N_{\text{pch},2\phi}(t)(z - \mu(t))$.

$$\rho_m(z,t) = 1 - \frac{\alpha(z,t)}{N_r}$$

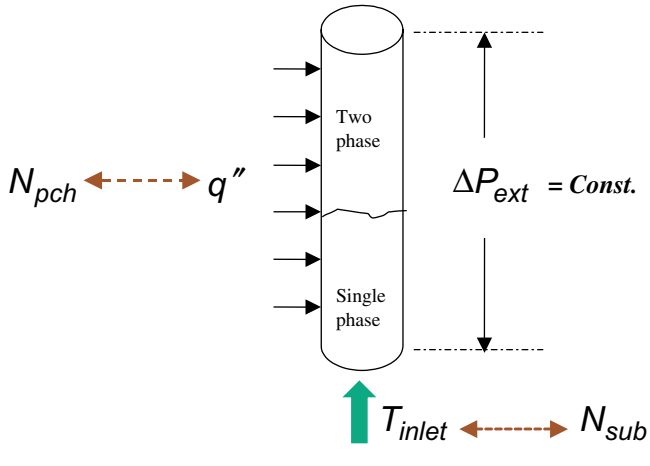

Fig. 1. A schematic view of a heated channel model.

is the mixture density, and

$$v_m(z,t) = j(z,t) + (V_{gj} + (C_0 - 1)j(z,t))\left(1 - \frac{1}{\rho_m(z,t)}\right)$$

is the mixture velocity.

The drift flux relation between the void fraction $\alpha(z,t)$ and the equilibrium quality $x(z,t)$ is

$$\alpha(z,t) = \frac{x(z,t)N_r}{C_0(x(z,t) + N_\rho N_r) + \dfrac{V_{gj}N_\rho N_r}{G}} \tag{8}$$

where G is the mass flow rate, and can be related to the quality by

$$G(z,t) = \frac{j(z,t)N_g}{x + (1 - x_{\text{eq}})N_\rho} = \frac{j(z,t)N_\rho N_r}{x + N_\rho N_r} \tag{9}$$

Equation (8) can be simplified to

$$\alpha(z,t) = \frac{x(z,t)j(z,t)N_r}{(x(z,t) + N_\rho N_r)(C_0 j(z,t) + V_{gj})} \tag{10}$$

The void fraction for the drift flux model can be written as a sum of the void fractions due to the homogeneous equilibrium model and a correction term:

$$\alpha(z,t) = \frac{1}{C_0}(\alpha_{\text{homo}}(z,t) - V_{gj} \cdot \alpha_{\text{corr}}(z,t)) \tag{11}$$

where

$$\alpha_{\text{homo}}(z,t) = \frac{x(z,t)N_r}{(x(z,t) + N_\rho N_r)}$$

and

$$\alpha_{\text{corr}}(z,t) = \frac{x(z,t)N_r}{(x(z,t) + N_\rho N_r)(C_0 j(z,t) + V_{gj})}.$$

Taking into account the quadratic dependence of the quality in the spatial direction [Karve *et al.*, 1994],

$$x(z,t) \approx N_\rho N_r[s_1(t)(z - \mu(t)) + s_2(t)(z - \mu(t))^2] \tag{12}$$

we substitute the values of $x(z,t)$ and $j(z,t)$ in Eq. (10), substitute the resulting Eq. (10) in the void propagation Eq. (6), and finally, using the weighted residuals method,[2] we obtain the ODEs for the phase variables in the two-phase region, $s_1(t)$ and $s_2(t)$, by integrating from the boiling boundary $z = \mu(t)$ to the channel exit $z = 1$:

$$\frac{ds_1(t)}{dt} = \frac{1}{ff_5(t)}\left[ff_1(t)\frac{d\mu(t)}{dt} + ff_2(t)\frac{dv_{\text{inlet}}(t)}{dt} + ff_3(t)\frac{dN_{\text{pch},2\phi}(t)}{dt} + ff_4(t)\right] \tag{13}$$

$$\frac{ds_2(t)}{dt} = \frac{1}{ff_{10}(t)}\left[ff_6(t)\frac{d\mu(t)}{dt} + ff_7(t)\frac{dv_{\text{inlet}}(t)}{dt} + ff_8(t)\frac{dN_{\text{pch},2\phi}(t)}{dt} + ff_9(t)\right] \tag{14}$$

where $s_1(t)$ and $s_2(t)$ are the coefficients of the linear and quadratic terms in the quality profile, and $ff_n(t) = 1, \ldots, 9$ are complicated intermediate quantities, which depend on the phase variables, the operating parameters and the design parameters. Since these expressions are very long [Dokhane, 2004], their detailed forms are not presented here.

Finally, using the fixed total pressure drop with respect to time as a boundary condition, the single-phase and two-phase momentum equations are used to derive the ODE for the inlet liquid velocity $v_{\text{inlet}}(t)$, which is one of the state variables. Integrating the momentum equations for the single-phase and two-phase regions, we get the equations for single and two-phase pressure drops ($\Delta P_{1\phi}$ and $\Delta P_{2\phi}$, respectively) in terms of $v_{\text{inlet}}(t)$. Finally, these pressure drops are summed along with the inlet and exit pressure drops (ΔP_{inlet} and ΔP_{exit}, respectively), and then set equal to the external pressure drop ΔP_{ext}:

$$\Delta P_{1\phi}(t) + \Delta P_{2\phi}(t) + \Delta P_{\text{inlet}}(t) + \Delta P_{\text{exit}}(t) = \Delta P_{\text{ext}} \tag{15}$$

Rearranging Eq. (15) leads to the equation for the inlet velocity

$$\frac{dv_{\text{inlet}}(t)}{dt} = \frac{1}{ff_{14}(t)}\left(ff_{11}(t)\frac{d\mu(t)}{dt} + ff_{12}(t)\frac{dN_{\text{pch},2\phi}}{dt} + ff_{13}(t)\right) \tag{16}$$

where $ff_n(t) = 11, \ldots, 14$ are complicated intermediate quantities, which depend on the phase variables, and the operating and the design parameters.

[2]The weight functions used to obtain ODEs for $s_1(t)$ and $s_2(t)$ are 1 and z.

2.3. *Summary of the model*

The dynamical system that results from the heated channel model can be written in a compact form as:

$$\dot{X}(t) = F(X;\kappa) \tag{17}$$

where $X(t) = (a_1(t), a_2(t), s_1(t), s_2(t), v_{\text{inlet}}(t))^T$ is the vector of phase variables, $a_1(t)$ and $a_2(t)$ are the coefficients of the linear and quadratic terms for the liquid enthalpy profile, $s_1(t)$ and $s_2(t)$ are the coefficients of the linear and quadratic terms for the quality profile, $v_{\text{inlet}}(t)$ is the liquid velocity at the channel inlet, and κ is the vector of parameters that includes both operating and design parameters

$$\kappa = (N_\rho, N_r, N_{\text{pch},1\phi}, N_{\text{pch},2\phi}, N_{\text{sub}}, K_{\text{inlet}}, K_{\text{exit}}, N_{f,1\phi}, N_{f,2\phi}, Fr, \Delta P_{\text{ext}}, C_0, V_{gj}). \tag{18}$$

It should be pointed out that, a validation study [Dokhane, 2004], not presented in this paper, in which the results of this model have been compared to the certain appropriate experimental data [Saha *et al.*, 1976] as well as to several earlier models developed to simulate two-phase flow instabilities [Ishii & Zuber, 1970; Saha & Zuber, 1978; Rizwan-uddin & Dorning, 1986; Dykhuizen *et al.*, 1986; Karve *et al.*, 1994], has shown that the current model is in fact in better agreement with the experimental data than most of the other models.

3. Methods

3.1. *Hopf bifurcation*

Hopf bifurcation has been reported by many researchers [Achard *et al.*, 1985; Rizwan-uddin & Dorning, 1986; Muñoz-Cobo & Verdú, 1991; Tsuji *et al.*, 1993; Karve *et al.*, 1997; van der Bragt *et al.*, 1999; Dokhane *et al.*, 2003] to be the most important type of bifurcation observed during heated channel and boiling water reactor (BWR) stability analysis. Generally speaking, Hopf bifurcation theory states that stable or unstable periodic solutions to a set of nonlinear differential equations exist under certain conditions. Consider the following system of ODEs

$$\frac{d\mathbf{x}(t)}{dt} = F(\mathbf{x}, \lambda) \tag{19}$$

where $\mathbf{x}(t)$ is the state vector, F an analytical vector function, and λ is the so-called bifurcation parameter. $\tilde{\mathbf{x}}$ is the steady-state solution or the fixed point of Eq. (19), i.e. $F(\tilde{\mathbf{x}}, \lambda) = 0$ for all λ.

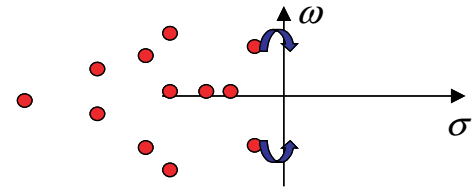

Fig. 2. Schematic illustration of the occurrence of Hopf bifurcation in the complex plane of Jacobian matrix eigenvalues.

The Hopf bifurcation theorem states that:

If

(i) a pair of complex conjugate eigenvalues $\sigma(\lambda) \pm i\omega(\lambda)$ of the Jacobian matrix crosses the imaginary axis for a critical value of $\lambda = \lambda_c$ in such a way that $\omega(\lambda_c) > 0$, $\sigma(\lambda_c) = 0$ and $\partial\sigma(\lambda = \lambda_c)/\partial\lambda \neq 0$, and,

(ii) all the other eigenvalues have strictly negative real parts (see Fig. 2),

then:

periodic solutions of Eq. (19) bifurcate from a branch of the steady-state solution x_{eq} at $\lambda = \lambda_c$.

In simpler terms, the theorem implies that periodic solutions to the nonlinear differential equations exist for parameter values λ if at $\lambda = \lambda_c$ a pair of complex conjugate eigenvalues of the Jacobian matrix has zero real part while all others are away from, and to the left of, the imaginary axis, and the derivative of the real part of the pair of eigenvalues on the imaginary axis with respect to λ is non-zero. These periodic solutions only exist either on the stable side or on the unstable side. If the periodic solutions exist on the unstable side of the SB, they are stable, and the Hopf bifurcation is called supercritical. On the other hand, if the periodic solutions exist on the stable side of the SB, they are unstable and the Hopf bifurcation is called subcritical.

The stability of the periodic solution is determined by applying the Floquet theory of differential equations with periodic coefficients [Nayfeh & Balachandran, 1995], in which two Floquet exponents appear to give more nonlinear information regarding the system stability behavior. The first exponent is always zero and the other exponent, β, determines the stability of the periodic oscillation. If $\beta < 0$, the periodic solution is stable (supercritical bifurcation), while if $\beta > 0$ the periodic solution is unstable (subcritical bifurcation). Since Floquet theory is based on linear analysis, the obtained

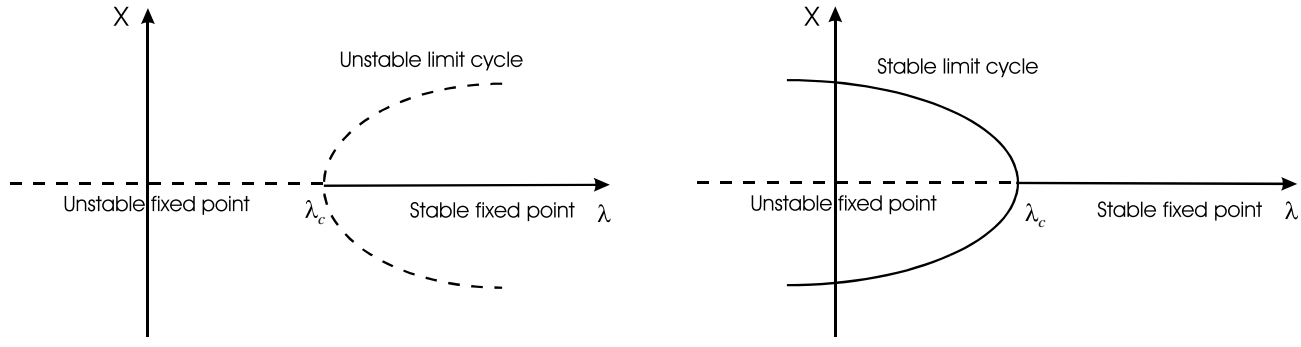

(a) Subcritical Hopf bifurcation

(b) Supercritical Hopf bifurcation

Fig. 3. Sub- and supercritical PAH bifurcations, unstable limit cycle for subcritical PAH bifurcation, and stable limit cycle for supercritical PAH bifurcation.

information on the periodic solutions is valid only close to the stability boundary.

Transition from a stable (unstable) fixed point solution to an unstable (stable) fixed point and a stable (unstable) periodic solution (limit cycle) is shown schematically in Fig. 3. The case of subcritical Hopf bifurcation, shown in Fig. 3(a), has an unstable periodic solution (repeller limit cycle) for $\lambda > \lambda_c$. Hence, for $\lambda > \lambda_c$, perturbations of amplitude less than the amplitude of the parabola will decay to zero (stable fixed point solution), while perturbations of amplitude greater than the limit cycle amplitude will be repelled and hence will move away from the stable fixed point as well as from the unstable limit cycle. On the other hand, in the supercritical Hopf bifurcation case shown in Fig. 3(b), there exist stable limit cycles in the unstable region, and hence small perturbations grow and stabilize at the limit cycle, while perturbations with amplitude larger than the limit cycle radius (amplitude) can decay onto the limit cycle, depending upon the size of the perturbation and the basin of attraction of the stable limit cycle.

3.2. *Semi-analytical bifurcation analysis*

Crossing a stability boundary between a region with no eigenvalues with positive real parts and a region with one pair of complex conjugate eigenvalues with positive real parts implies Hopf bifurcation. Such a stability boundary can be easily determined via a linear analysis. However, to determine the nature of bifurcation (sub- versus supercritical) and the oscillation amplitude close to the stability boundary, additional (bifurcation) analyses are necessary. Such bifurcation studies are usually performed in one of two ways, viz. either by numerically integrating the set of governing equations, or analytically. However, due to the limitations of both approaches, as discussed in Sec. 1, an alternative approach has currently been adopted in which analytical bifurcation is carried out numerically. In this approach, the governing set of nonlinear equations are neither integrated numerically in time nor treated entirely analytically. Rather, the analytical reduction to the Poincaré normal form *via* the center manifold theorem is carried out numerically [Hassard, 1986]. This approach, which henceforth is called the *semi-analytical* method, allows accurate and efficient evaluation of the entire parameter space of interest.

3.3. *Bifurcation code BIFDD*

The bifurcation code BIFDD (Bifurcation Formulae for Delay-Differential system) was developed by Hassard [1987] to perform semi-analytical bifurcation analysis of sets of ODEs and ODEs with delays. This code has been used in the current work to analyze the stability and bifurcation characteristics of the newly developed heated channel model in the design and operating parameter space. For a given set of nonlinear ODEs or ODEs with delays and the corresponding Jacobian matrix, the code determines the critical value of the bifurcation parameter λ_c, the frequency and amplitude of the oscillation, and the parameters μ_2, τ_2 and β_2. A negative (positive) value of β_2 indicates a supercritical (subcritical) Hopf bifurcation. τ_2 is a correction factor for the oscillation frequency, and μ_2 relates the oscillation amplitude to the value of the bifurcation parameter. By incrementally varying a second parameter and repeating the calculations for the

critical value of the bifurcation parameter, one can easily generate stability boundaries and determine the nature of the bifurcation along such boundaries in two-dimensional parameter spaces.

In the present context, a main Fortran program has been developed, which calls BIFDD and employs a special subroutine written to provide the right-hand side of the set of nonlinear ODEs, as well as the Jacobian matrix, derived using the symbolic toolbox Maple.

4. Results and Discussions

4.1. *Semi-analytical bifurcation analysis*

The aim in this section is to carry out a comparative analysis between the use of DFM and HEM using semi-analytical bifurcation analysis with the code BIFDD. Results for stability boundaries are presented here in the subcooling number — phase change number ($N_{\text{sub}} - N_{\text{pch}}$)[3] operational parameter plane, because it is in this plane that the validation of the current model has been carried out against experimental data [Dokhane, 2004]. Typical numerical values used in this research for the design and operating parameters are given in Appendix B.

Drift Flux Model versus Homogeneous Equilibrium Model

By setting $C_0 = 1$ and $V_{gj} = 0$, the present model reduces to the homogeneous equilibrium model (HEM) as used by Karve *et al.* [1994]. Shown in Fig. 4 are the stability and bifurcation results for the HEM ($C_0 = 1$ and $V_{gj} = 0$) and the DFM with $C_0 = 1.03$ and $V_{gj} = 0.1$. The stability boundaries in the $N_{\text{sub}} - N_{\text{pch}}$ plane are shown in Fig. 4(a). This figure clearly shows that the SB is sensitive to the model used. The corresponding bifurcation diagram in the $N_{\text{sub}} - \beta_2$ plane shows that both sub- and super-critical Hopf bifurcations are encountered. (As mentioned in Sec. 3.3, β_2 is a parameter[4] in the bifurcation analysis. $\beta_2 < 0$ implies supercritical Hopf bifurcation, while $\beta_2 > 0$ indicates subcritical Hopf bifurcation.) In this case, Hopf bifurcation is subcritical ($\beta_2 > 0$) for $N_{\text{sub}} < 3.15$, and supercritical ($\beta_2 < 0$) for higher values of N_{sub} [see Fig. 4(b)]. Referring to Fig. 4(b), points A, B and C shown in Fig. 4(a) are located in the region where subcritical bifurcation is predicted when crossing the SB, while

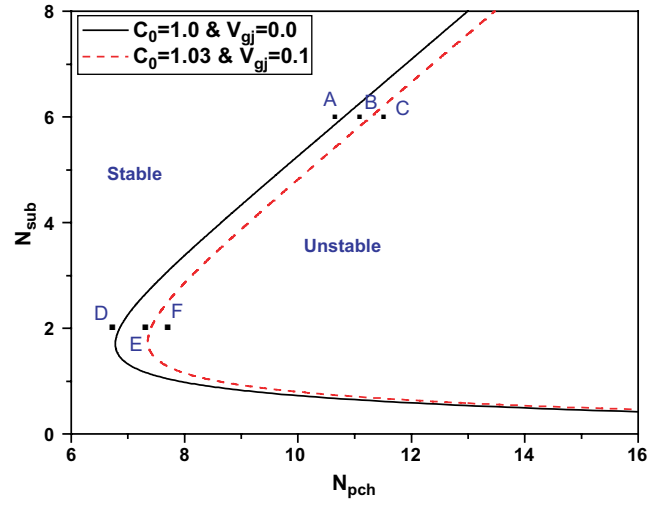

(a)

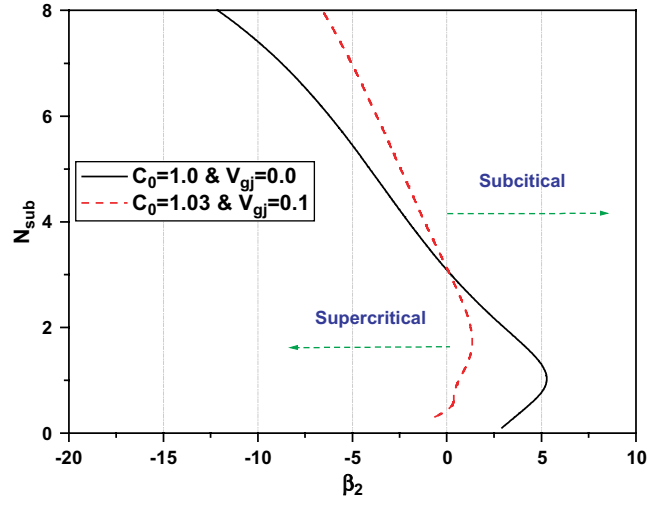

(b)

Fig. 4. (a) Stability boundaries in $N_{\text{sub}} - N_{\text{pch}}$ plane for Homogeneous Equilibrium Model (HEM) and Drift Flux Model (DFM). (b) Nature of Hopf bifurcation in $N_{\text{sub}} - \beta_2$ plane for HEM and DFM. Bifurcation is supercritical for $\beta_2 < 0$, and subcritical for $\beta_2 > 0$.

points D, E and F are located in the region where subcritical bifurcation is expected.

In references [Achard *et al.*, 1985] and [Rizwanuddin & Dorning, 1986], however, it was reported that only supercritical Hopf bifurcation is encountered in the above parameter range. This disagreement in the bifurcation results may be ascribed to differences in the assumptions made in the

[3] N_{pch} is here the two-phase change number, i.e. $N_{\text{pch},2\phi}$ (see Appendix A).
[4] β_2 is related to β [Hassard, 1987] through $\beta = \varepsilon^2\beta_2$, where ε is the oscillation amplitude.

individual models. It would seem, therefore, that further investigations are needed to clarify this discrepancy. For instance, a study that evaluates the effects of using other simplifying assumptions (e.g. those made in models of Clausse and Lahey [1991] and Karve *et al.* [1994]) on the nature of Hopf bifurcation would help considerably to understand this disagreement.

The effects of the drift flux model parameters (C_0 and V_{gj}) on the stability as well as on the bifurcation characteristics are investigated next. While the stability boundary is sensitive to the value of C_0 ($V_{gj} = 0$), as seen in Fig. 5(a), the nature of Hopf bifurcation is less affected. Only a small shift of the transition point between the sub- and supercritical regions is observed as C_0 changes from 1.0 to 1.03 [Fig. 5(b)]. For example, the transition occurs at $N_{\text{sub}} = 3.15$ for HEM, at $N_{\text{sub}} = 3.4$ for DFM with $C_0 = 1.03$ and $V_{gj} = 0$, and at $N_{\text{sub}} = 3.65$ for $C_0 = 1.05$ and $V_{gj} = 0$. As was reported earlier by Rizwan-uddin and Dorning [1986], C_0 is seen to have a stabilizing effect [Fig. 5(a)]. This can be explained qualitatively by the following: for $C_0 > 1$, the concentration of bubbles at the periphery of the heated channel is lower than that for HEM. This causes less friction in the two-phase region, which

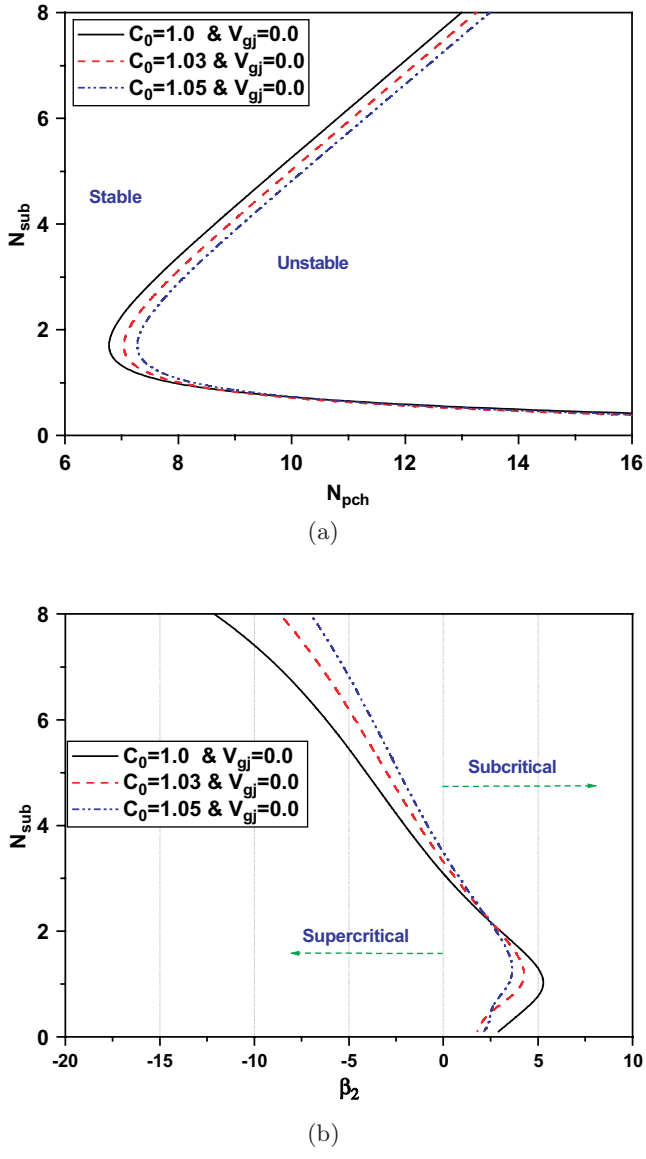

Fig. 5. Effects of C_0 variations. (a) Stability boundaries in $N_{\text{sub}}-N_{\text{pch}}$ plane. (b) Nature of Hopf bifurcation in $N_{\text{sub}}-\beta_2$ plane. Bifurcation is supercritical for $\beta_2 < 0$, and subcritical for $\beta_2 > 0$.

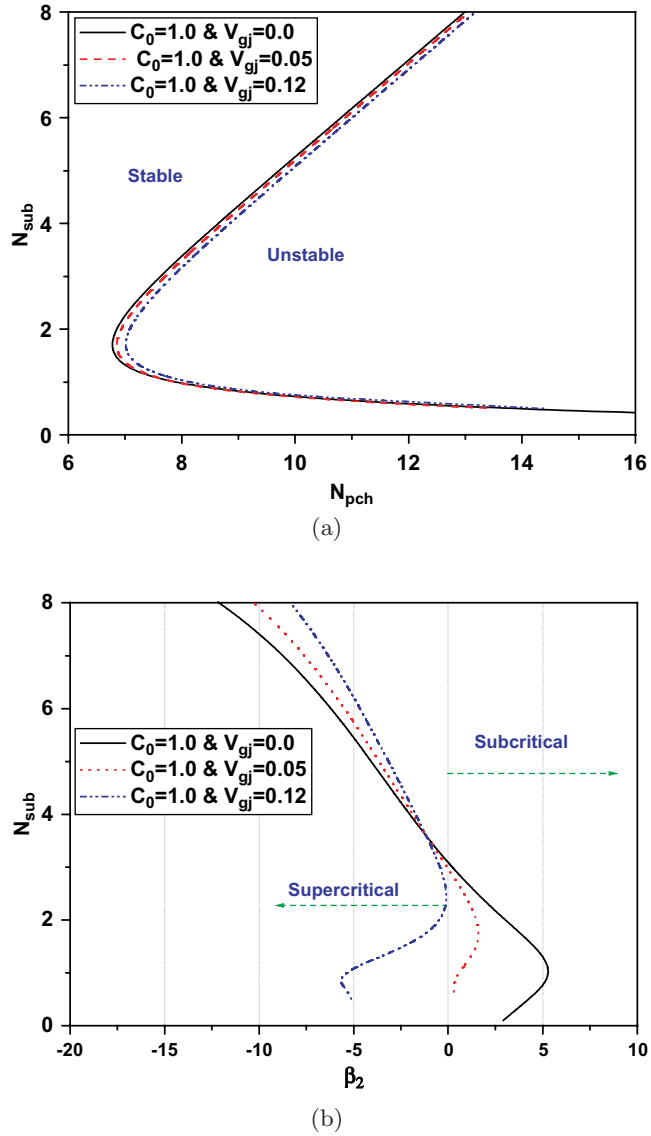

Fig. 6. Effects of V_{gj} variations. (a) Stability boundaries in $N_{\text{sub}}-N_{\text{pch}}$ plane. (b) Nature of Hopf bifurcation in $N_{\text{sub}}-\beta_2$ plane. Bifurcation is supercritical for $\beta_2 < 0$, and subcritical for $\beta_2 > 0$.

means a lower two-phase region pressure drop; thus, the heated channel is more stable.

Results on the effects of the drift velocity V_{gj} are presented in Fig. 6. The SB is a little less sensitive to the value of V_{gj} [Fig. 6(a)] than it is to typical values of C_0 [Fig. 5(a)]. However, the nature of Hopf bifurcation for lower values of N_{sub} is more sensitive to the value of V_{gj}. For example, for $V_{gj} = 0.12$ ($C_0 = 1$), the branch of the SB which was subcritical in the HEM case disappears and the entire SB becomes supercritical [Fig. 6(b)]. Like C_0, V_{gj} also has a stabilizing effect. The reason is that, for $V_{gj} > 0$, the velocity of the liquid is less than the mixture velocity in the HEM. This results in a decrease of the two-phase pressure drop that stabilizes the system. Although there is a partly compensating effect due to the steam velocity being higher than the mixture velocity in the HEM, the contribution of the liquid phase to the pressure drop is greater than that of the gas phase.

It should be noted that, although the stabilizing effects of C_0 and V_{gj} are well understood, explaining the effects of these two parameters on the bifurcation characteristics remains a challenge.

4.2. *Numerical simulation*

It needs to be pointed out that bifurcation analyses of the above type are only valid in the vicinity of the SB. Hence, numerical integration of the set of five ODEs has been carried out — in the MATLAB environment — to confirm the predictions of the semi-analytical bifurcation analyses close to the SB, as well as to provide global information beyond the local bifurcation findings, i.e. to evaluate the system behavior in regions away from the SB. For the numerical integration of the ODEs, a fifth order Runge–Kutta method has been used.

Figures 7–9 show, respectively, the time evolution of the inlet velocity with parameter values corresponding to points A, B and C — in the supercritical region — shown in Fig. 4(a). As expected, the point A is stable for both the HEM and DFM [Fig. 4(a)]. Hence, the oscillation amplitude decays

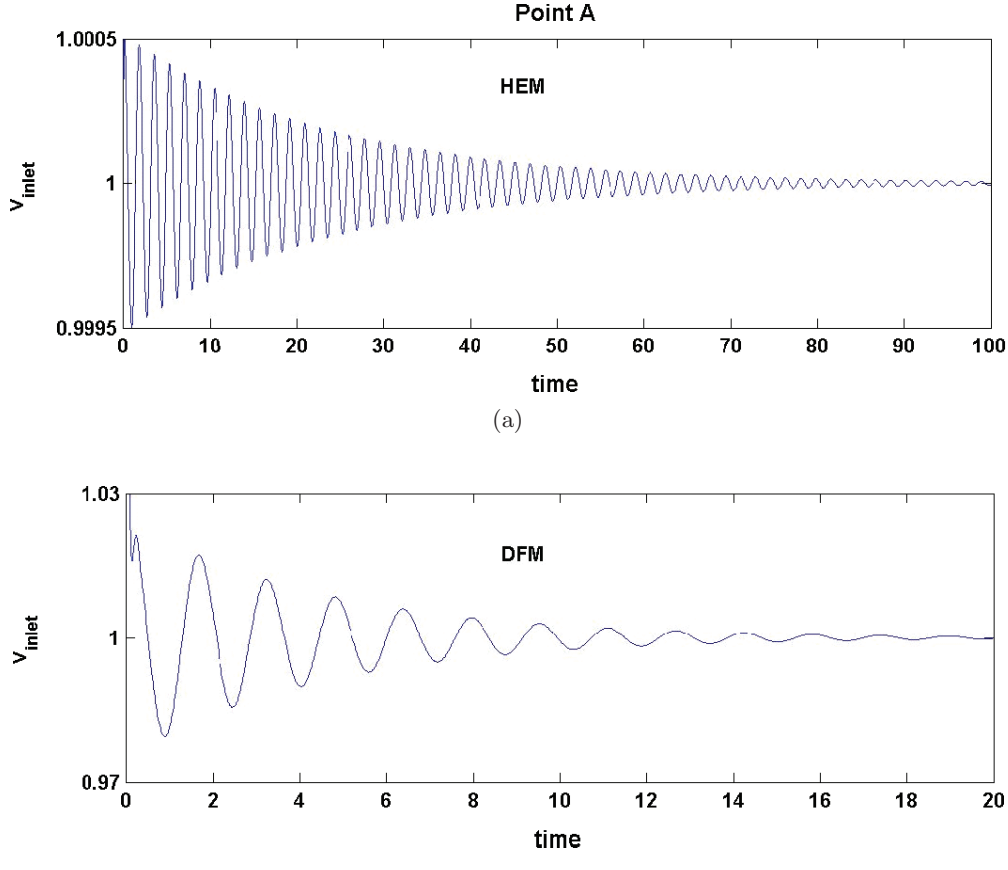

Fig. 7. Time evolution of liquid inlet velocity $v_{\text{inlet}}(t)$ for parameter values corresponding to point A for: (a) Homogeneous Equilibrium Model (HEM), (b) Drift Flux Model (DFM).

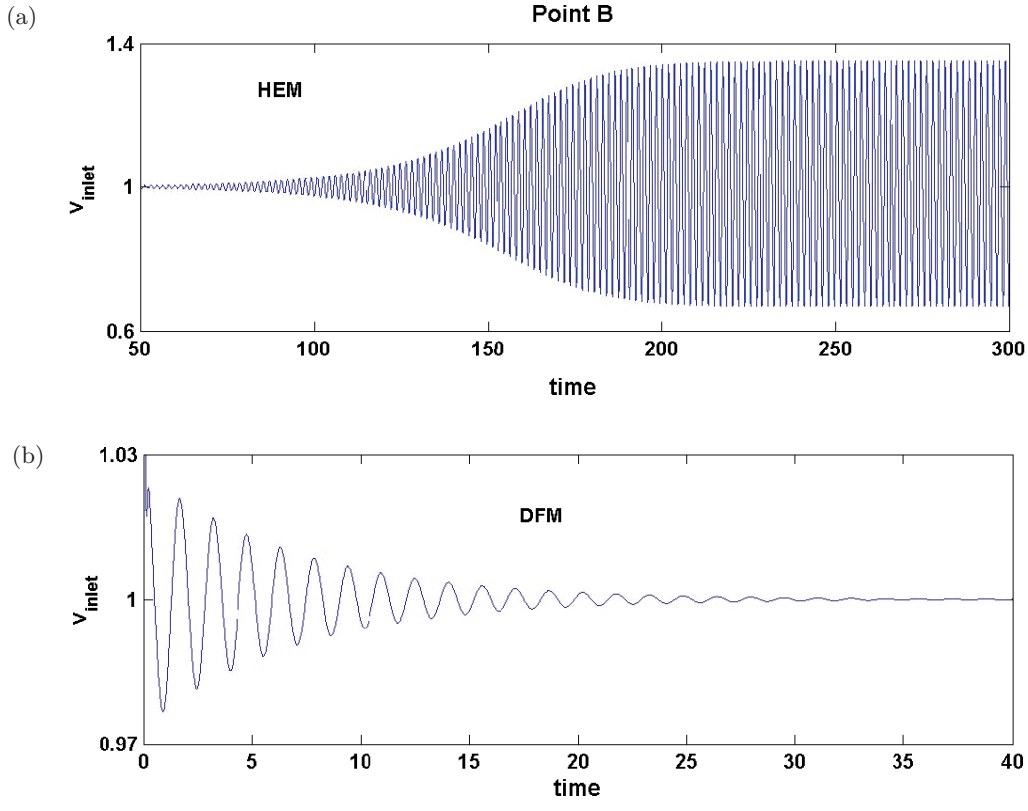

Fig. 8. Time evolution of liquid inlet velocity $v_{\text{inlet}}(t)$ for parameter values corresponding to point B for: (a) Homogeneous Equilibrium Model (HEM), (b) Drift Flux Model (DFM).

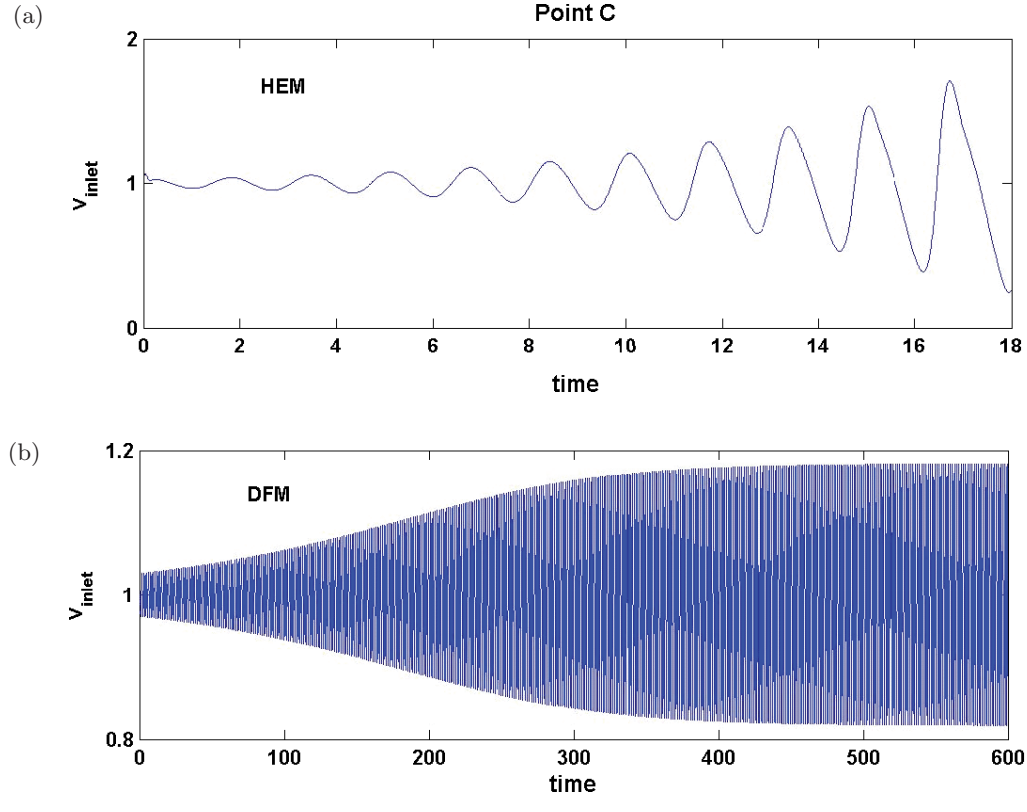

Fig. 9. Time evolution of liquid inlet velocity $v_{\text{inlet}}(t)$ for parameter values corresponding to point C for: (a) Homogeneous Equilibrium Model (HEM), (b) Drift Flux Model (DFM).

to the fixed point [Figs. 7(a) and 7(b)]. Point B, shown in Fig. 4(a), is in the unstable region for the HEM. It is close to the stability boundary and the nature of Hopf bifurcation is supercritical. Therefore, as predicted by the bifurcation analysis, this leads to stable limit cycle oscillations, as shown in Fig. 8(a). However, point B is stable for the DFM, and consequently the oscillation amplitude decays to the fixed point [Fig. 8(b)]. Finally, point C is in the unstable region and it is far from the SB for the HEM [Fig. 4(a)]. Therefore, the oscillation amplitude grows away from the fixed point [Fig. 9(a)]. However, for the DFM case, point C is in the unstable region but close to the SB. Hence, this leads to a stable limit cycle, as shown in Fig. 9(b).

Figures 10–12 show, respectively, the system dynamics at points D, E and F, shown in Fig. 4(a). Point D is in the stable region for both models. In addition, it is close to the SB for the HEM, and the type of Hopf bifurcation is subcritical. Therefore, beside the stable fixed point, an unstable limit cycle is predicted. Numerical simulations confirm these findings, as shown in Figs. 10(a) and 10(b). The small amplitude perturbation ($\delta s_2 = 0.1$) decays to the fixed point [Fig. 10(a)], and the large amplitude perturbation ($\delta s_2 = 5.0$) leads to growing amplitude oscillations [Fig. 10(b)]. For the DFM [Fig. 10(c)], however, point D is far enough from the SB so that only decaying oscillations are encountered, i.e. only a fixed-point attractor exists.

Numerical integration results with parameter values corresponding to point E are shown in Fig. 11. This point is on the unstable side for the HEM, so that the system evolves with growing amplitude oscillations [Fig. 11(a)]. However, for the DFM, since point E is on the stable side and close to the SB, and the nature of Hopf bifurcation is subcritical, a fixed point attractor for small amplitude perturbations around the fixed point and an unstable limit cycle for large perturbation amplitude are

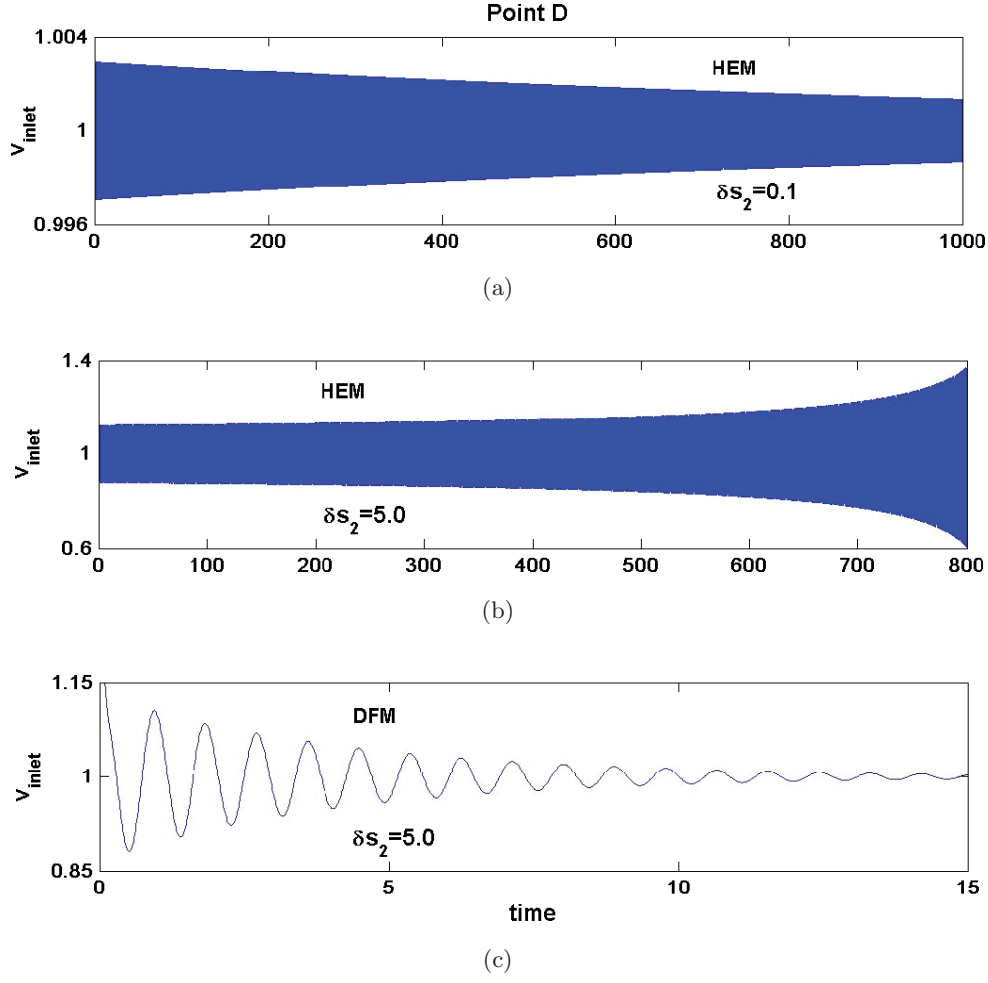

Fig. 10. Time evolution of liquid inlet velocity $v_{\text{inlet}}(t)$ for parameter values corresponding to point D for: (a)–(b) Homogeneous Equilibrium Model (HEM) with, respectively, small and large perturbation amplitudes, (c) Drift Flux Model (DFM).

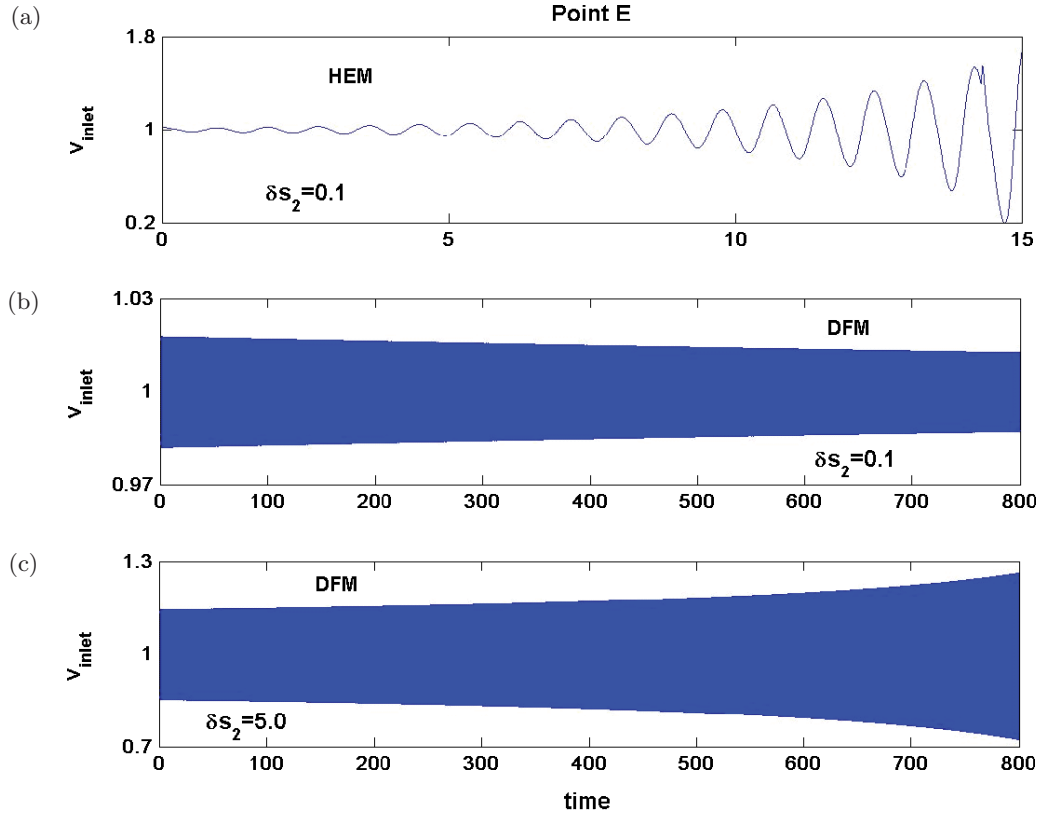

Fig. 11. Time evolution of liquid inlet velocity $v_{\text{inlet}}(t)$ for parameter values corresponding to point E for: (a) Homogeneous Equilibrium Model (HEM), (b)–(c) Drift Flux Model (DFM) with small and large perturbation amplitudes, respectively.

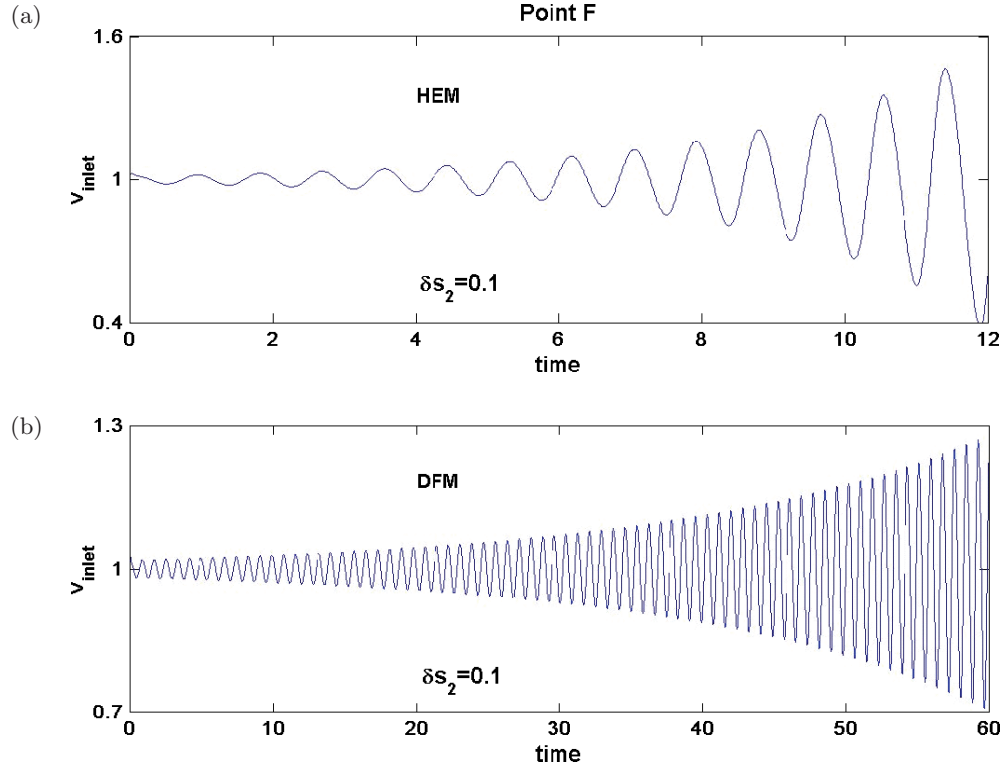

Fig. 12. Time evolution of liquid inlet velocity $v_{\text{inlet}}(t)$ for parameter values corresponding to point F for: (a) Homogeneous Equilibrium Model (HEM), (b) Drift Flux Model (DFM).

predicted by the bifurcation analysis. Numerical simulations confirm these predictions [Figs. 11(b) and 11(c)]. Finally, point F is a trivial unstable fixed point for both models, and Figs. 12(a) and 12(b) show its dynamics.

It should be noted that, in the case of subcritical Hopf bifurcation, the strip close to the SB where unstable limit cycles exist is very narrow. However, for the supercritical case, the strip that comprises stable limit cycles is quite wide. This means that it is much easier to identify a stable limit cycle than an unstable limit cycle.

5. Summary and Conclusions

A new model for two-phase flow in a heated channel has been developed using a drift flux representation. Stability and semi-analytical bifurcation analyses have been performed using the bifurcation analysis code BIFDD, stability boundaries and bifurcation characteristics being determined in the $N_{\text{sub}} - N_{\text{pch}}$ operational space. The results of the bifurcation analysis along these stability boundaries clearly show that both sub- and super-critical Hopf bifurcations can be expected. The impact of the parameters of the drift flux model (C_0 and V_{gj}) has been investigated in this context. While the SB is found to be sensitive to values of both C_0 and V_{gj}, the nature of Hopf bifurcation for lower values of N_{sub} is found to be considerably more sensitive to the value of V_{gj}. The above results have been confirmed by numerical integration of the set of ODEs.

Acknowledgments

The authors would like to express their appreciation to J. F. Stubbins, Head of the Department of Nuclear, Plasma, and Radiological Engineering at the University of Illinois (UIUC), for the warm hospitality received by the first author during his stay at UIUC.

BWR stability research at PSI forms part of the nuclear safety analysis project STARS at PSI, and the authors would like to thank M. A. Zimmermann, the STARS project manager, for support and discussions. This work has been partly sponsored by the Swiss Federal Nuclear Safety Inspectorate.

References

Achard, J. L., Drew, L. A. & Lahey, R. T. [1985] "The analysis of nonlinear density-wave oscillations in boiling channels," *J. Fluid Mech.* **155**, 213–232.

Clausse, A. & Lahey, R. T. [1991] "The analysis of periodic and strange attractors during density-wave oscillations in boiling flows," *Chaos Solit. Fract.* **1**, 167–178.

Dokhane, A., Hennig, D., Rizwan-uddin & Chawla, R. [2003] "Nuclear-coupled thermal-hydraulic nonlinear stability analysis using a novel BWR reduced order model: Part 1 — The effect of using drift flux versus homogeneous equilibrium models," *Proc. 11th Int. Conf. Nuclear Engineering* (ICONE11), Tokyo, Japan, 20–23 April, CD-ROM.

Dokhane, A. [2004] "BWR stability and bifurcation analysis using a novel reduced order model and the system code RAMONA," Doctoral Thesis No. 2927, EPFL, Switzerland, 2004.

Dykhuizen, R. C., Roy, R. P. & Kalra, S. P. [1986] "A linear time-domain two-fluid model analysis of the dynamic instability in boiling flow systems," *J. Heat Transfer* **108**, p. 222.

Hassard, B. D. [1986] *Dynamics of Nonlinear Systems* (Gordon and Breach), Chap. 9.

Hassard, B. D. [1987] "A code for Hopf bifurcation analysis of autonomous delay-differential equations," in *Proc. Oscillation, Bifurcation and Chaos*, Canadian Mathematical Society, pp. 447–463.

Ishii, M. & Zuber, N. [1970] "Thermally induced flow instabilities in two-phase mixtures," *Heat Transfer* **V**, p. B11.

Jensen, P. J. & Galer, R. R. [1990] "Analysis of water level reduction during ATWS/instability events," in *Proc. Int. Workshop on BWR Stability*, OECD/NEA CSNI Report 178, pp. 446–456.

Karve, A. A., Rizwan-uddin & Dorning, J. J. [1994] "On spatial approximations for liquid enthalpy and two-phase quality during density wave oscillations," *Trans. Am. Nucl. Soc.* **71**, p. 533.

Karve, A. A., Rizwan-uddin & Dorning, J. J. [1997] "Stability analysis of BWR nuclear-coupled thermal-hydraulics using a simple model," *Nucl. Eng. Des.* **177**, 155–177.

Muñoz-Cobo, J. L. & Verdú, G. [1991] "Application of Hopf bifurcation theory and variational methods to the study of limit cycles in boiling water reactors," *Ann. Nucl. Energy* **18**, p. 269.

Nayfeh, A. H. & Balachandran, B. [1995] *Applied Nonlinear Dynamics: Analytical, Computational, and Experimental Methods* (John Wiley, NY).

Rizwan-uddin & Dorning, J. J. [1986] "Some nonlinear dynamics of a heated channel," *Nucl. Eng. Des.* **93**, 1–14.

Saha, P., Ishii, M. & Zuber, N. [1976] "An experimental investigation of thermally induced flow oscillations in two-phase systems," *J. Heat Transfer* **98**, 616–622.

Saha, P. & Zuber, N. [1978] "An analytical study of the thermally induced two-phase flow instabilities

including the effect of thermal non-equilibrium," *Int. J. Heat Mass Transfer* **21**, 415–426.
Tsuji, M., Nishio, K. & Narita, M. [1993] "Stability analysis of BWRs using bifurcation theory," *J. Nucl. Sci. Tech.* **30**, 1107–1119.
van der Bragt, D. D. B., Rizwan-uddin & van der Hagen, T. H. J. J. [1999] "Nonlinear analysis of a natural circulation boiling water reactor," *Nucl. Sci. Eng.* **131**, 23–44.
Wulf, W., Cheng, H. S., Diamond, D. J. & Khatib-Rahbar, M. [1984] "A description and assessment of RAMONA-3B Mod. 0 Cycle 4: A computer code with three-dimensional neutron kinetics for BWR system transients," NUREG/CR-3664.
Zuber, N. & Staub, F. W. [1967] "An analytical investigation of the transient response of the volumetric concentration in a boiling forced-flow system," *Nucl. Sci. Eng.* **30**, p. 268.

Nomenclature

A	cross-sectional flow area
C_0	void distribution parameter
D	diameter
DFM	drift flux model
Fr	Froude number
HEM	homogeneous equilibrium model
N_f	friction number
N_{sub}	subcooling number
N_{pch}	phase change number
K_{exit}	exit pressure loss coefficient
K_{inlet}	inlet pressure loss coefficient
PAH	Poincaré–Andronov–Hopf
T_{inlet}	liquid inlet temperature
ΔP	pressure drop
SB	stability boundary
V_{gj}	void drift velocity
f	friction factor
g	gravitational constant
h	enthalpy
j	volumetric flow rate
L	channel length
q''	wall heat flux
p	pressure
v	velocity
x	equilibrium quality
Γ	void generation rate
α	void fraction
μ	position of the boiling boundary
ρ	density
ξ	heated perimeter

Subscripts

corr	correction
ext	external
homo	homogeneous
f	liquid
g	vapor
m	mixture
1ϕ	single-phase
2ϕ	two phase

Superscripts

$*$	dimensional quantity
$\sim$	steady state value

Appendix A

The dimensionless variables and parameters in the single and two-phase regions are:

$$\Delta P_{\text{ext}} = \frac{\Delta P^*_{\text{ext}}}{\rho^*_f v^{*2}_0} \qquad \Gamma = \frac{q''^* \xi^* L^*}{A^* \Delta h^*_{fg} v^*_0 \rho^*_g}$$

$$v = \frac{v^*}{v^*_0} \qquad \rho_m = \frac{\rho^*_m}{\rho^*_f}$$

$$\mu = \frac{\mu^*}{L^*} \qquad j = \frac{j^*}{v^*_0}$$

$$V_{gj} = \frac{V^*_{gj}}{v^*_0} \qquad z = \frac{z^*}{L^*}$$

$$Fr = \frac{v^{*2}_0}{g^* L^*} \qquad N_{f,j\phi} = \frac{f_{j\phi} L^*}{2 D^*_h}$$

$$N_\rho = \frac{\rho^*_g}{\Delta \rho^*} \qquad N_r = \frac{\rho^*_f}{\Delta \rho^*}$$

$$N_{\text{pch}} = \frac{q''^* \xi^* L^* \Delta \rho^*}{A^* \Delta h^*_{fg} \rho^*_g \rho^*_f v^*_0} \qquad N_{\text{sub}} = \frac{(h^*_{\text{sat}} - h^*_{\text{inlet}}) \Delta \rho^*}{\Delta h^*_{fg} \rho^*_g}$$

Appendix B

Results presented in this paper were obtained using the following numerical values for the design and operating parameters.

$$Fr = 0.03333 \qquad K_{\text{exit}} = 2.0 \qquad K_{\text{inlet}} = 6.0$$

$$N_{f,1\phi} = 2.8 \qquad N_{f,2\phi} = 5.6 \qquad N_r = 1.05397$$

$$N_\rho = 0.05120$$